

# Differences in the Dominant Modes of the Interannual Variability of Eastern Tibetan Plateau Precipitation between Early and Peak Summers



Erfan Liu<sup>1</sup>, Song Yang<sup>1,2</sup>, Haolin Luo<sup>3</sup>, Jiehong Xie<sup>1</sup>, Ziqian Wang<sup>1,2</sup>

<sup>1</sup> School of Atmospheric Sciences, Sun Yat-sen University, and Southern Marine Science and Engineering Guangdong Laboratory (Zhuhai), Zhuhai, China

<sup>2</sup> Guangdong Province Key Laboratory for Climate Change and Natural Disaster Studies, Sun Yat-sen University, Zhuhai, China

<sup>3</sup> Department of Atmospheric Sciences, Climate Change and Resource Utilization in Complex Terrain Regions Key Laboratory of Sichuan Province, Chengdu University of Information Technology, Chengdu, China

liuerf@mail2.sysu.edu.cn

## 1. Introduction

### Why It Matters

Precipitation variation on the TP directly regulates the local and downstream water resources, and changes the local atmospheric heat source.

### What We Don't Know

Are the dominant interannual variability modes of summer precipitation consistent between early summer (June) and peak summer (July–August)? Does a mode transition exist?

### What we do

Using multi-source observations, reanalysis, and CESM simulations, we reveal the intraseasonal transition mechanism of ETP summer precipitation from a dipole to a monopole pattern.

## 2. Data & Methods

**Data:** CN05.1, APHRODITE, GPCP, GPCP, JRA-55 (1979–2022).

**Methods:** EOF/MV-EOF, sliding spatial correlation, moisture budget,

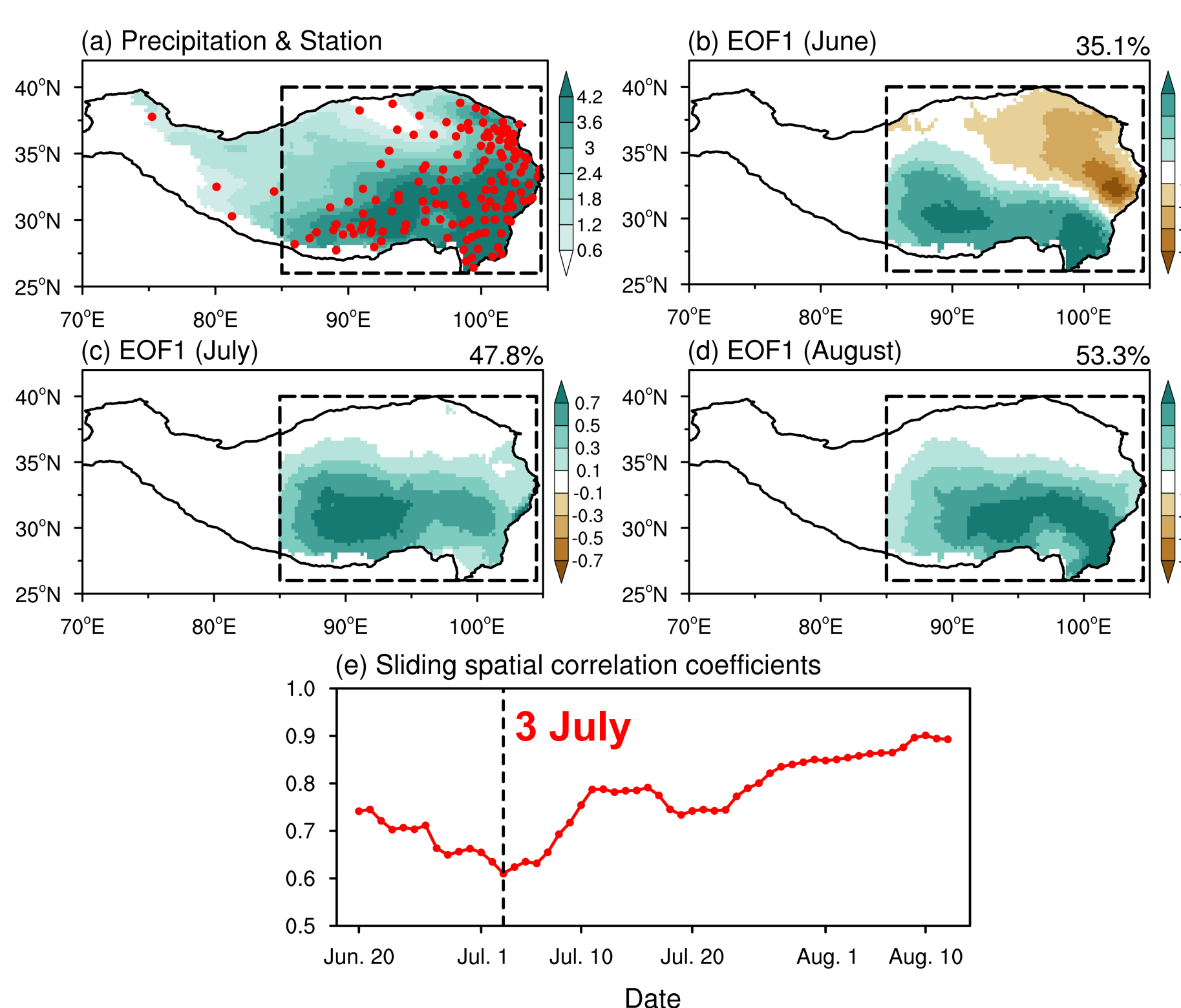
$$P' = E' - \langle \bar{u} \partial_x q' \rangle - \langle \bar{v} \partial_y q' \rangle - \langle \bar{\omega} \partial_p q' \rangle - \langle u' \partial_x \bar{q} \rangle - \langle v' \partial_y \bar{q} \rangle - \langle \omega' \partial_p \bar{q} \rangle + NL + \text{Residual},$$

MSE budget,

$$\langle \omega' \partial_p \bar{h} \rangle \approx F'_{net} - \langle u' \partial_x (C_p \bar{T} + L_v \bar{q}) \rangle - \langle \bar{u} \partial_x (C_p T + L_v q) \rangle - \langle v' \partial_y (C_p \bar{T} + L_v \bar{q}) \rangle - \langle \bar{v} \partial_y (C_p T + L_v q) \rangle - \langle \bar{\omega} \partial_p \bar{h}' \rangle + NL,$$

**Model:** CAM4 (CESM1.2.2), SASM\_heat sensitivity experiment.

## 3. Intraseasonal Differences



The north-south dipole pattern only clearly appears and remains stable in June. In July and August, the dominant modes show a monopole pattern.

The dominant modes before and after 3 July are the most inconsistent.

## 4. Early Summer (June) - Dipole pattern

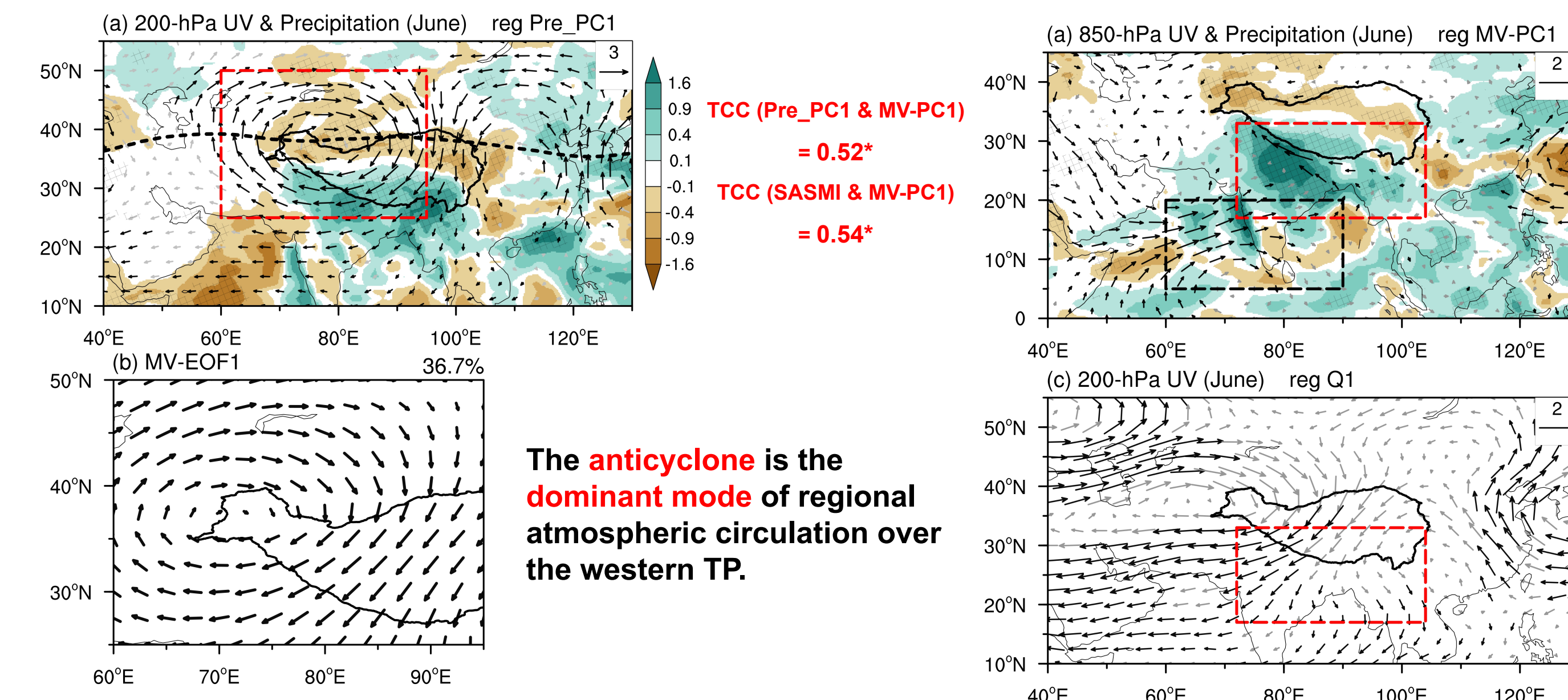


Fig. 2. (Left) Regressions of 200-hPa horizontal winds and precipitation onto the PC1 of the interannual variability of ETP precipitation in June, along with the dominant mode of atmospheric circulation.

Fig. 3. (Right) Regression of 850-hPa horizontal winds and precipitation onto the MV-PC1 of the horizontal winds over the western TP in June.

The anticyclone is the dominant mode of regional atmospheric circulation over the western TP.

The SASM convective heating can force a large-scale anomalous anticyclonic circulation over the upper levels to the northwest of the heating as a Gill-type response.

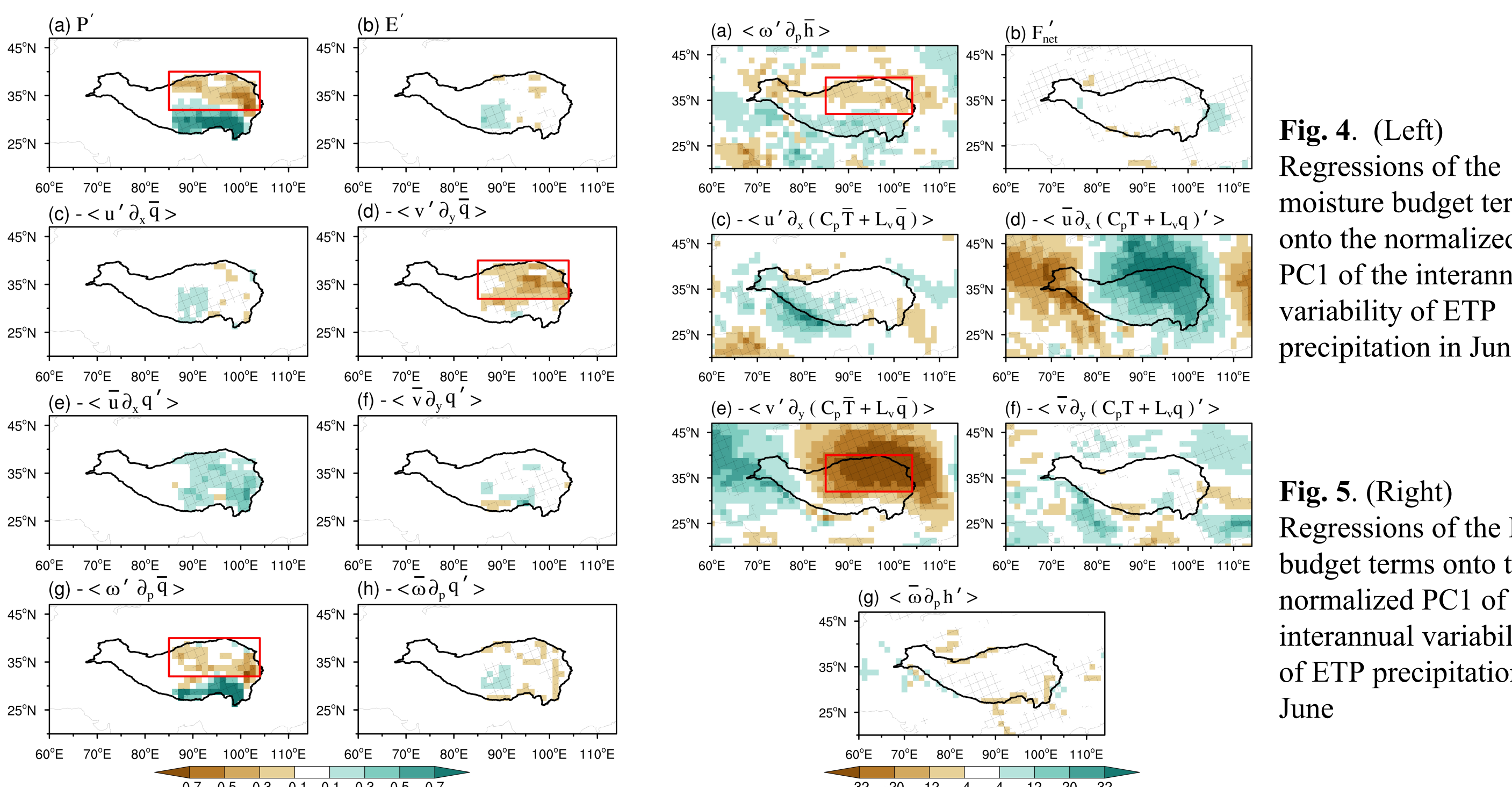


Fig. 4. (Left) Regressions of the moisture budget terms onto the normalized PC1 of the interannual variability of ETP precipitation in June

Fig. 5. (Right) Regressions of the MSE budget terms onto the normalized PC1 of the interannual variability of ETP precipitation in June

Under the influence of anomalous northerlies, negative moisture advection and moist enthalpy advection are transported into the northern ETP, where reduced moisture and anomalous sinking motions jointly lead to negative precipitation anomalies

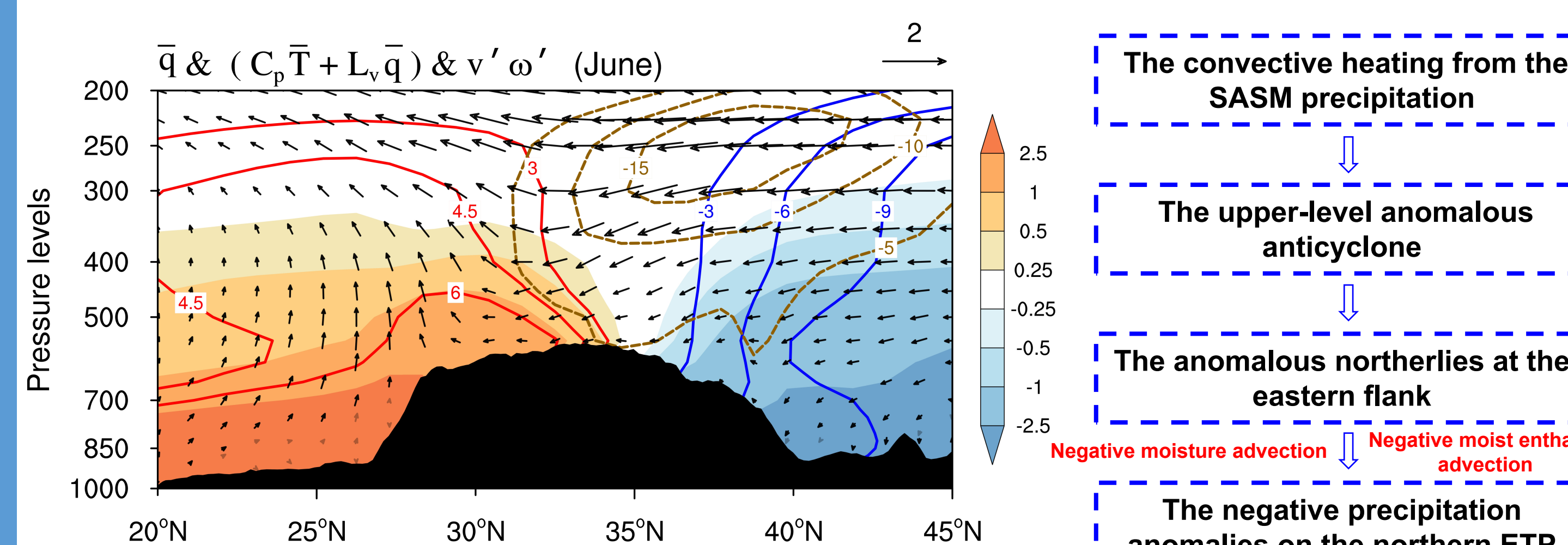


Fig. 6. The meridional distribution of climatological specific humidity (shading) and moist enthalpy (red (+) and blue (-) contours) and regressions of the circulation onto the PC1 of the interannual variability of ETP precipitation in June.

## 5. Peak Summer (July–August) - Monopole pattern

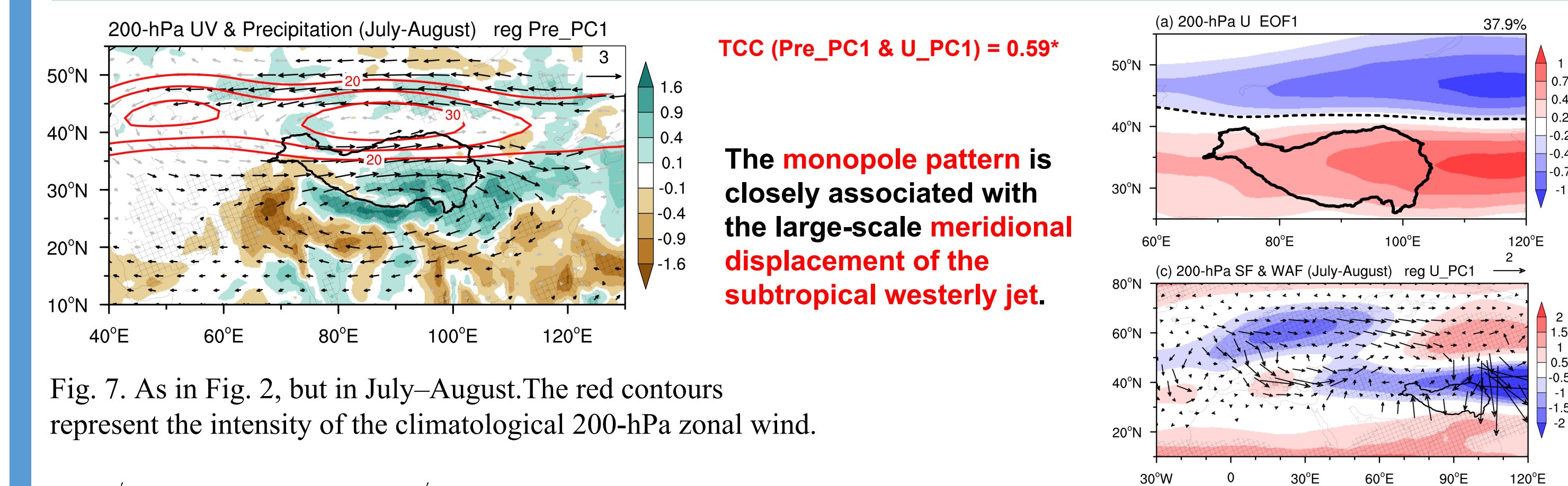


Fig. 7. As in Fig. 2, but in July–August. The red contours represent the intensity of the climatological 200-hPa zonal wind.

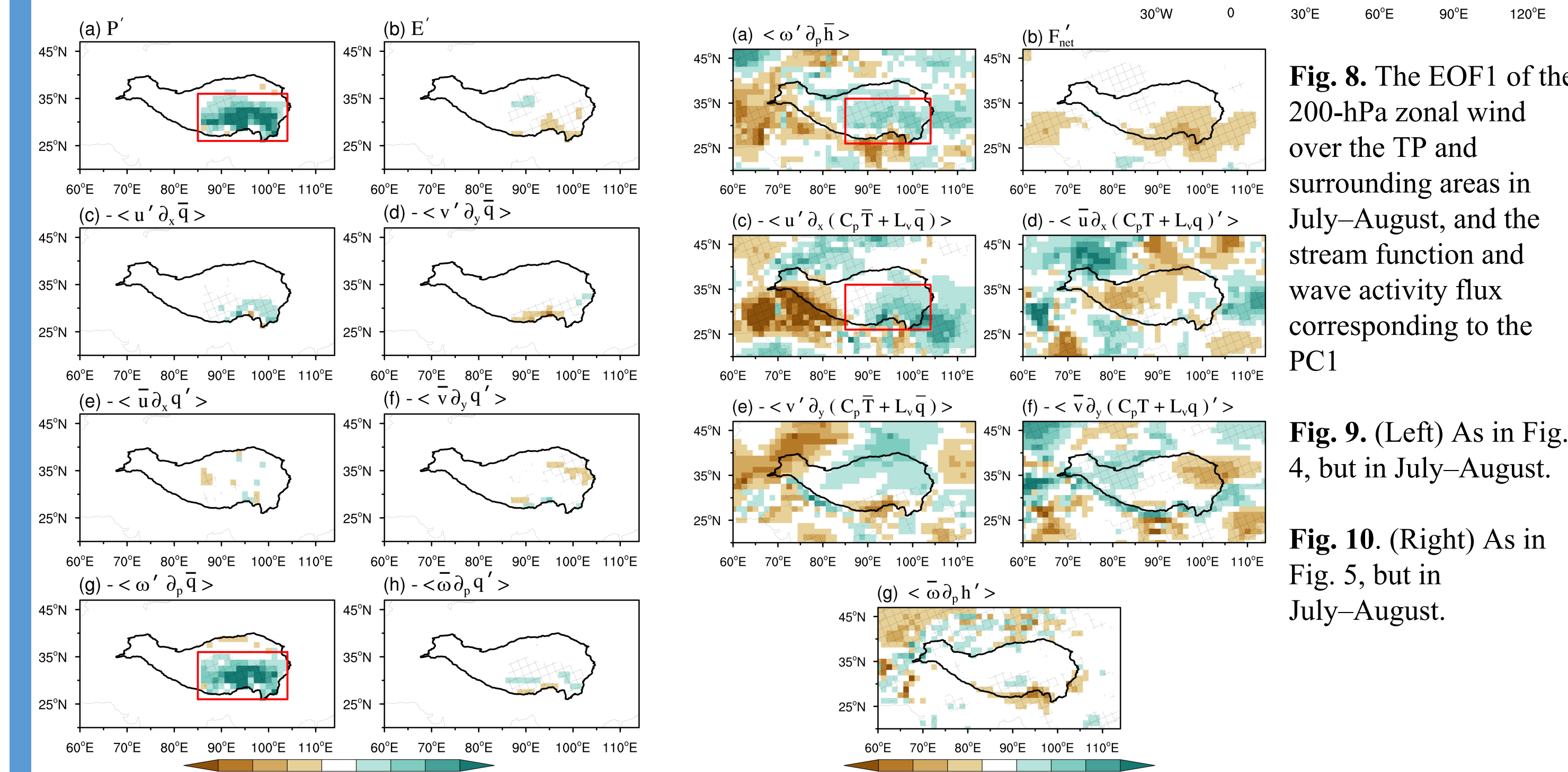


Fig. 8. The EOF1 of the 200-hPa zonal wind over the TP and surrounding areas in July–August, and the stream function and wave activity flux corresponding to the PC1

Fig. 9. (Left) As in Fig. 4, but in July–August.

Fig. 10. (Right) As in Fig. 5, but in July–August.

Positive moist enthalpy anomalies are transported into the ETP, triggering anomalous upward motions and then leading to overall consistently positive precipitation anomalies.

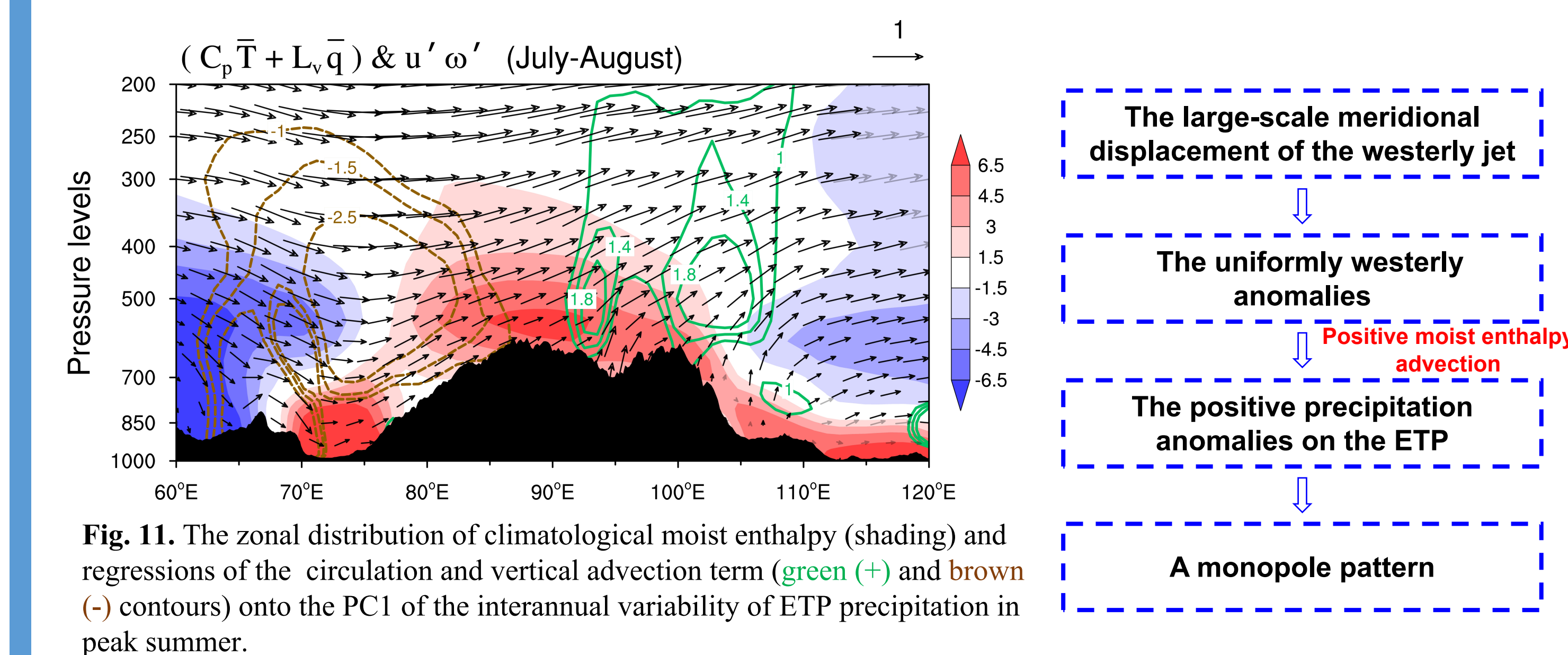


Fig. 11. The zonal distribution of climatological moist enthalpy (shading) and regressions of the circulation and vertical advection term (green (+) and brown (-) contours) onto the PC1 of the interannual variability of ETP precipitation in peak summer.

## 6. Conclusions

- The dominant mode of ETP summer precipitation shifts from a dipole pattern to a monopole pattern.
- The dipole pattern in June is driven by SASM convective heating that produces northerlies of anomalous anticyclonic circulation and sinking motion over northern ETP.
- The monopole pattern in July–August is controlled by meridional shifts of the westerly jet that generate westerlies and rising motion over the whole ETP.